J. Fluid Mech. (1990), *vol.* 211, *pp.* 373–392
Printed in Great Britain

Spreading and instability of a viscous fluid sheet

By L. M. HOCKING
Department of Mathematics, University College London, Gower Street, London WC1E 6BT, UK

(Received 28 November 1988 and in revised form 31 July 1989)

Experiments by Huppert (1982) have demonstrated that a finite volume of fluid placed on an inclined plane will elongate into a thin sheet of fluid as it slides down the plane. If the fluid is initially placed uniformly across the plane, the sheet retains its two-dimensionality for some time, but when it has become sufficiently long and thin, the leading edge develops a spanwise instability. A similarity solution for this motion was derived by Huppert, without taking account of the edge regions where surface tension is important. When these regions are examined, it is found that the conditions at the edges can be satisfied, but only when the singularity associated with the moving contact line is removed. When the sheet is sufficiently elongated, the profile of the free surface shows an upward bulge near the leading edge. It is suggested that the observed instability of the shape of the leading edge is a result of the dynamics of the fluid in this bulge. The related problem of a ridge of fluid sliding down the plane is examined and found to be linearly unstable. The spanwise lengthscale of this instability is, however, dependent on the width of the channel occupied by the fluid, which is at variance with the observed nature of the instability. Preliminary numerical solutions for the nonlinear development of a small disturbance to the position of a straight leading edge show the incipient development of a finger of fluid with a width that does not depend on the channel size, in accordance with the observations.

1. Introduction

Consider a fixed volume of fluid initially placed uniformly across an inclined plane and held there. When the fluid is released, it slides down the plane under gravity in the form of an elongating and thinning sheet. If the leading edge of the sheet is straight when the fluid is released, and if it remains straight throughout the motion, the whole surface of the plane will eventually be coated by the fluid. An exception to this outcome will occur if the contact angle of the fluid and the total fluid volume are such that a static equilibrium can be reached, with the whole fluid supported by the resolved surface tension at the leading edge. If this is not the case, then the quantity of interest is the speed of the leading edge of the fluid as it moves down the plane. It is by no means certain, however, that the hypothesis that the leading edge should remain straight throughout the motion is justified. If the motion is unstable to small spanwise disturbances to the position of the leading edge, the nonlinear development of these distortions may well result in the plane being only partially covered by the fluid. It is clearly of some importance to determine the circumstances in which such a failure to achieve a complete coating can occur.

Experiments on the spreading of a fixed amount of viscous fluid have been reported by Huppert (1982). He derived a similarity solution governing the

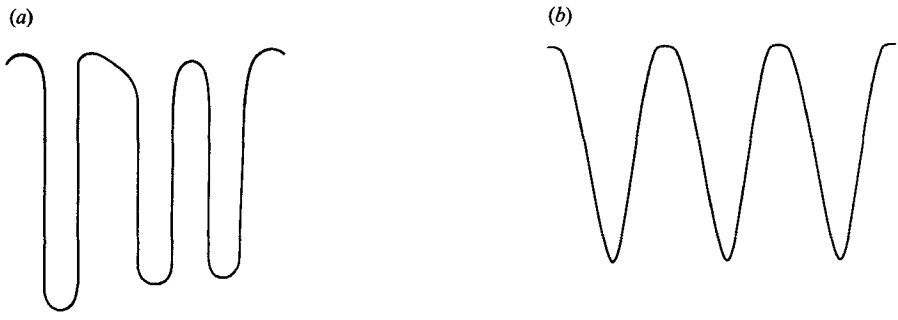

FIGURE 1. The two types of instability: (*a*) parallel-sided fingers, (*b*) triangles.

viscosity–gravity balance when the fluid has been stretched sufficiently far that lubrication theory can be applied, and his experiments provided convincing evidence that this similarity solution was valid; the length of the sheet is proportional to the cube root of the elapsed time. Surface tension must, however, be important near the leading edge of the sheet (and, to a lesser degree, at the upper edge also). The similarity solution gives a non-zero thickness for the sheet at its lower extremity. The good agreement between the similarity solution and the experimental evidence suggests, however, that the bulk motion of the fluid is unaffected by the details of the dynamics in the vicinity of the leading edge.

Huppert's experiments also showed that, when the sheet of fluid had become long enough, and correspondingly thin, the leading edge spontaneously developed a spanwise and roughly periodic variation. Measurements of the wavelength of this variation for different fluids showed that it does depend on the surface tension, unlike the stretching motion of the sheet, but no explanation of the nature of the instability nor why it only became manifest some time after the fluid had been released were presented. An interesting phenomenon concerning the nature of the spanwise variations was observed when the initial instability had developed to a finite amplitude. In some cases the leading edge took the form of a series of triangles, with both the bases and the tips moving down the plane. The tips, however, moved faster than the bases so that the triangles lengthened as time went on. In other cases, parallel-sided fingers of equal width but irregularly spaced were found; the tips moved down the plane but the bases of the fingers and the fluid remaining in the continuous sheet above them were stationary. These two types of instability are sketched in figure 1. Silvi & Dussan V. (1985) point out an important consequence of the difference between these two types. For the triangular form, as for the sheet without any instability, the whole plane will eventually be covered by the fluid. If the parallel-sided fingers appear, then the regions of the plane between them will remain uncoated by the fluid. In Huppert's experiments, using fluids with differing viscosities and surface tensions, both types were encountered, but there did not seem any obvious correlation between the properties of the fluids and the type of the instability. Silvi & Dussan V. repeated the experiments of Huppert, but instead of using different fluids on the same substrate, they used the same fluid on two different substrates. Thus the viscosity and surface tension were unchanged, but the contact angles between the fluid and the substance forming the plane on which the sheet was moving differed. They found that, with glass and a contact angle of 18°, triangles were formed, but with Plexiglas and a contact angle of 70°, the parallel-sided fingers emerged. This clearly suggests that, in order to predict which type of instability will

occur, it is necessary to pay close attention to the dynamics of the fluid near the moving contact line.

There are three goals to the investigation to be described in the present paper. The first is to show that it is possible to complete the description of the motion given by Huppert's similarity solution to include the vicinity of the edges. An attempt to do so was given by Huppert, but it is based on an incorrect equation. The second is to identify the reason for the delayed appearance of the instability. The third is to find the characteristics of a linear instability of the leading edge. There is a fourth goal, which is only partially achieved in this paper. It is to find the form of the instability that will be present when the infinitesimal disturbances of the linear theory have grown to a finite size. This nonlinear theory will be needed to explain the distinction between the two types that are observed, the triangles and the parallel-sided fingers. Numerical evidence tentatively suggests the formation of the fingers, but does not support the appearance of triangular shapes for the leading edge. More extensive numerical work currently in progress will, it is hoped, achieve this fourth goal more satisfactorily.

Throughout this paper we shall be dealing with fluid sheets that are long compared with their depth. Huppert's experiments reveal, as will be demonstrated later, that the instability begins when the capillary number is small. (The capillary number measures the relative importance of viscous and capillary forces.) This is an important point, because the characteristics of the flow near the front of an advancing sheet depend significantly on the size of the capillary number. When the capillary number is large, as at the head of a gravity-driven current, the fluid advances in a sort of rolling manner, with air entrainment under the leading edge and with rapid variations of velocity within the front. At low capillary numbers, however, the flow is quite different. The advance is quasi-steady and there is a well-defined contact line which moves along the plane surface. In the present case the capillary number is very small and it is essential, therefore, to include effects that are important when moving contact lines are present, such as contact-angle variation and the removal of the force singularity there. Because we are dealing with long thin sheets of fluid, it is natural to wish to make use of lubrication theory. Thus we shall not be able to describe the initial stages of the motion, when the fluid is held at the top of the plane. We shall also have to restrict attention to fluids and solids that have a small mutual contact angle, since lubrication theory requires the slope of the free surface of the fluid relative to the plane substrate to be small. In order to bridge the gap between the contact line and the similarity solution for the main part of the sheet, surface tension must be included but this does not permit an acceptable solution unless there is slip at the contact line. This should cause no surprise since it is well known that such an adjustment to the standard boundary condition is needed in the vicinity of moving contact lines. The precise form of condition that is used is not important; a variety of models for this condition have been proposed (see Dussan V. 1976), but they all produce comparable results. The application of this condition enables a satisfactory solution to be obtained, and shows that, for small capillary numbers, the head of the sheet bulges upwards to a height that is several times the height of the sheet behind the head. The presence of such an increase in height of in the frontal region above that of the leading sheet was not reported by Huppert in his experiments, though it has been observed in sliding motions of fluid at low capillary numbers and is a common feature of theoretical investigations of such flows (Hocking 1981). In an extreme form, it can be seen on any window on a wet day; the water forming the bulk of a drop that is slipping down the glass leaves behind it a thin film

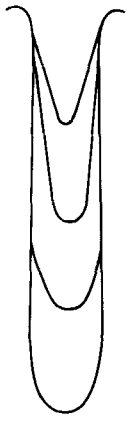

FIGURE 2. Evolution of triangles into parallel-sided fingers.

of water. The reason for the presence of this bulge is presumably the competition of gravity pulling the fluid down and the reluctance of the contact line to move, leading to a build-up of fluid immediately behind the head. The presence of this bulge suggests that the instability may be associated with the part of the fluid near the head, with the remainder of the sheet playing only a passive role. If this be so, then we can simplfy the problem, retaining the important dynamical processes, by considering a ridge of fluid near the leading edge and ignoring the presence of the thin sheet stretching back from the bulge to the top of the plane. The spreading and sliding of such a ridge was the subject of earlier papers (Hocking 1981, 1982). A linear stability analysis has now been done and it shows that spanwise variations in the position of the edges of such a ridge are unstable and that the maximum growth rate is associated with the longest wave that can fit into the region between the bounding sides of the channel occupied by the fluid. The fluid tends to collect towards one side or other of the channel and move down the plane there. This is not the instability that is observed, however, and we must go on to consider the nonlinear development of an initial disturbance to the leading edge. The numerical solution so far attempted is not conclusive, but it does point towards the development of a finger of fluid moving down the plane with a width that is independent of the width of the channel. Hence it appears that the simplified model problem of the ridge does account for the development of the parallel-sided fingers of equal width and unequal spacing that are observed in some of the experiments.

These results give no hint of the appearance of the triangular form found in some of the experiments. In this mode, the contact line has a non-zero velocity component normal to itself, so the contact angle is above its maximum static value. As the triangle lengthens this angle will decrease, so the triangular form cannot exist indefinitely. When the static value is reached, the fluid can only move in a direction parallel to the static contact line (Dussan V. & Chow 1983), and the pattern of the contact line may change into that of the parallel-sided fingers, in a manner like that sketched in figure 2. Thus, if we have a plane that is sufficiently long, the presence of the triangular shape will be only a transitory phenomenon and eventually, in all cases, parallel-sided fingers will develop. If this argument is correct, we might expect to see triangles more readily when the maximum static contact angle is small than when it is large, and their replacement by fingers requires the plane to be long enough. This is not inconsistent with the experiments of Silvi & Dussan V., as far as

the presence of triangles is concerned. But their conclusion that the size of the contact angle determines whether or not the plane is completely wetted by the fluid must be replaced by a condition combining both the contact angle (strictly the maximum static angle) and the length of the plane. Since the numerical work so far undertaken does not exhibit the triangular form, it is not yet possible to formulate this proposed condition.

2. Governing equations and parameters

It is convenient to formulate the problem in the most general form that will be used here, even though at first only a restricted case will be considered. Lubrication theory will be used throughout, so that the depth of the fluid is small compared with the lengthscale of variations in the depth, and we include spanwise variations, slip, contact angle hysteresis, and velocity-dependent contact angles.

Suppose that a volume V' of fluid is initially placed uniformly across a sloping plane and held there by a barrier. The plane is at an angle θ below the horizontal and the spanwise extent of the fluid is d'. When the barrier is removed, the fluid moves down the plane in the form of an elongating sheet which, some time after the fluid is released, becomes thin enough for lubrication theory to be applied. We shall ignore the initial stage of the motion as it will not have any lasting effect on the subsequent motion. The fluid is characterized by its density ρ, viscosity μ and surface tension γ, all of which are assumed to be constant, and g is the gravitational acceleration. Let (x', y', z') be Cartesian coordinates with their origin at the top of the plane and with x' measured down the plane, z' normal to the plane and y' horizontal, and let the corresponding velocity components be (u', v', w'). Then, if p' is the pressure in the fluid and t' is the time, the lubrication equations have the form

$$\frac{\partial p'}{\partial x'} - \rho g \sin\theta = \mu \frac{\partial^2 u'}{\partial z'^2}, \tag{1}$$

$$\frac{\partial p'}{\partial y'} = \mu \frac{\partial^2 v'}{\partial z'^2}, \tag{2}$$

$$\frac{\partial p'}{\partial z'} + \rho g \cos\theta = 0, \tag{3}$$

$$\frac{\partial u'}{\partial x'} + \frac{\partial v'}{\partial y'} + \frac{\partial w'}{\partial z'} = 0. \tag{4}$$

The height of the free surface of the fluid above the plane is denoted by $h'(x', y', t')$, The contact lines are where $h' = 0$ and, in their vicinity, we must allow for slip to occur when they are moving. A suitable form of boundary condition there is to suppose that the relative velocity between the fluid and the plane is proportional to the shear stress. Therefore, on the plane $z' = 0$,

$$u' = \tfrac{1}{3}\lambda' \frac{\partial u'}{\partial z'}, \quad v' = \tfrac{1}{3}\lambda' \frac{\partial v'}{\partial z'}, \quad w' = 0, \tag{5}$$

where $\frac{1}{3}\lambda'$ is the slip length and is much smaller than the height of the fluid. These conditions can be applied not only near the contact line but, for convenience, at all points covered by the fluid, the errors so introduced being no more than of order λ'/h' in magnitude.

On the free surface of the fluid, we have zero shear stress, constant normal stress and a kinematic condition for the fluid particles lying in the surface. These conditions are expressed by the following equations:

$$\frac{\partial u'}{\partial z'} = 0, \quad \frac{\partial v'}{\partial z'} = 0, \tag{6}$$

$$p' + \gamma\left(\frac{\partial^2 h'}{\partial x'^2} + \frac{\partial^2 h'}{\partial y'^2}\right) = p'_0, \tag{7}$$

$$\frac{\partial h'}{\partial t'} + u'\frac{\partial h'}{\partial x'} + v'\frac{\partial h'}{\partial y'} = 0, \tag{8}$$

where p'_0 is the atmospheric pressure.

The fluid is bounded in the spanwise direction by the planes $y' = 0, y' = d'$. If these are rigid boundaries, there will be boundary layers present on them, but these we shall ignore. We shall also want to deal with the case of an unbounded sheet with a spanwise variation of period $2d'$. In either case, we can apply the following conditions:

$$v' = \frac{\partial u'}{\partial y'} = \frac{\partial h'}{\partial y'} = \frac{\partial p'}{\partial y'} = 0 \quad \text{on} \quad y' = 0, d'. \tag{9}$$

The leading and trailing edges of the fluid are given by

$$x' = a'(y', t'), \quad x' = b'(y', t'), \quad 0 \leqslant y' \leqslant d', \tag{10}$$

and

$$h' = 0 \quad \text{at} \quad x' = a', \quad x' = b'. \tag{11}$$

If the top edge remains in its original position, $b' \equiv 0$, and, to maintain periodicity in the spanwise direction, we must have

$$\frac{\partial a'}{\partial y'} = \frac{\partial b'}{\partial y'} = 0 \quad \text{at} \quad y' = 0, d'. \tag{12}$$

The volume of the fluid remains constant during the motion so that there is an integral constraint on h' which can be expressed as follows:

$$\int_0^{d'} \int_{b'}^{a'} h'(x', y', t')\, \mathrm{d}x'\, \mathrm{d}y' = V'. \tag{13}$$

Finally, we need to postulate the contact angles at the two edges. If these angles are denoted by $\alpha(y', t')$ and $\beta(y', t')$ at the leading and trailing edges, respectively, we have

$$\tan\alpha = -\frac{\partial h'}{\partial n'}\bigg|_{x'=a'}, \quad \tan\beta = -\frac{\partial h'}{\partial n'}\bigg|_{x'=b'}, \tag{14}$$

where n' is normal to the contact line and is directed away from the fluid. Since we are using lubrication theory the gradients of h' are small, and we can replace $\tan\alpha$ by α and $\tan\beta$ by β. These contact angles are not fixed properties of the materials used, but vary with the motion as sketched in figure 3, where α_s and β_s are the maximum and minimum static contact angles (see Dussan V. 1979). For a fluid without contact angle hysteresis, $\alpha_s = \beta_s$, while for a completely wetting fluid, $\beta_s = 0$. For moving contact lines, the apparent contact angle, measured away from the vicinity of the slip region, is increased above the maximum static angle for a contact line moving forward and is decreased below the minimum static angle for backward motion. If

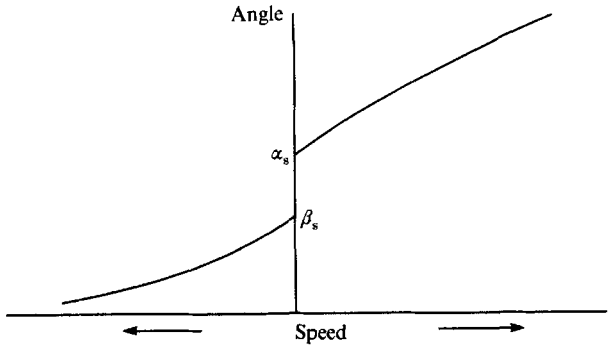

FIGURE 3. Contact-angle hysteresis and variation.

the capillary number is small enough, we can assume a linear variation with the speed. Let $U'_{a'}$ and $U'_{b'}$ be the normal velocity components of the contact lines, so that

$$U'_{a'} = \frac{\partial a'}{\partial t'}\left\{1+\left(\frac{\partial a'}{\partial y'}\right)^2\right\}^{-\frac{1}{2}}, \quad U'_{b'} = \frac{\partial b'}{\partial t'}\left\{1+\left(\frac{\partial b'}{\partial y'}\right)^2\right\}^{-\frac{1}{2}}. \tag{15}$$

Then, if δ' is the slope of the linear variation of the contact angles, we can express them as follows:

$$\left.\begin{aligned} \alpha &= \alpha_s + \delta' U'_{a'}, && \text{if } U'_{a'} > 0, \\ \beta_s \leqslant \alpha &\leqslant \alpha_s, && \text{if } U'_{a'} = 0, \\ \alpha &= \beta_s + \delta' U'_{a'}, && \text{if } U'_{a'} < 0, \end{aligned}\right\} \tag{16}$$

for the lower, leading edge of the fluid, and

$$\left.\begin{aligned} \beta &= \beta_s - \delta' U'_{a'}, && \text{if } U'_{b'} > 0, \\ \beta_s \leqslant \beta &\leqslant \alpha_s, && \text{if } U'_{b'} = 0, \\ \beta &= \alpha_s - \delta' U'_{a'}, && \text{if } U'_{b'} < 0, \end{aligned}\right\} \tag{17}$$

for the upper, trailing edge. We require, of course, that α and β be non-negative since the fluid is above the plane. If $\beta_s = 0$, the upper edge does not move from its initial position.

This completes the formulation of the problem, and, if we are given an initial state consistent with the lubrication approximation, we can use these equations and conditions to determine the evolution of the system. It is convenient to non-dimensionalize the variables at this stage. We define a lengthscale a_0 and a time scale t_0 by

$$a_0 = \left(\frac{V'}{d'}\right)^{\frac{1}{2}}, \quad t_0 = \frac{\mu}{\rho g a_0 \sin\theta}, \tag{18}$$

and the corresponding velocity scale is a_0/t_0. Non-dimensional quantities will be denoted by dropping the prime from the previously defined values. The solution of the lubrication equations is standard and the details need not be repeated here. The goal is an equation for the height h of the fluid, and this is found to take the following form:

$$3\frac{\partial h}{\partial t} + \left[\frac{\partial}{\partial x}\left\{h^2(h+\lambda)\frac{\partial}{\partial x}\right\} + \frac{\partial}{\partial y}\left\{h^2(h+\lambda)\frac{\partial}{\partial y}\right\}\right]\left[\sigma\left(\frac{\partial^2 h}{\partial x^2}+\frac{\partial^2 h}{\partial y^2}\right) - \cot\theta\, h\right] + \frac{\partial}{\partial x}\{h^2(h+\lambda)\} = 0. \tag{19}$$

The important dynamical parameter is σ, defined by

$$\sigma = \frac{\gamma}{\rho g a_0^2} \sin\theta . \tag{20}$$

The first term in (19) results from the viscous fluid motion, the term with factor σ represents the effect of surface tension, the term multiplied by $\cot\theta$ comes from the hydrostatic pressure across the depth of the fluid and the last term is the forcing term produced by the component of the weight of the fluid down the plane. In the spreading of fluid on a horizontal plane (Hocking 1983), only the first of the two gravitational terms is present, but on an inclined plane the second usually outweighs the first. The equation for $h(x,y,t)$ must be solved in the region $0 < y < d$, $b(y,t) < x < a(y,t)$, subject to the boundary conditions

$$h = 0 \quad \text{on} \quad x = b, a; \quad \frac{\partial h}{\partial y} = \frac{\partial^3 h}{\partial y^3} = 0 \quad \text{on} \quad y = 0, d; \tag{21}$$

we must also satisfy the volume constraint (13) in its non-dimensional form,

$$\int_0^d \int_b^a h \, \mathrm{d}x \, \mathrm{d}y = d. \tag{22}$$

The edge conditions are given by (16) and (17), with all the primes removed; since δ' is the reciprocal of a velocity, $\delta = \delta' a_0/t_0$. The parameter σ is an inverse Bond number, and in the experiments had a small value. Another parameter to which surface tension contributes is the capillary number $Ca = \mu U/\gamma$, where U is a typical velocity, which represents the relative importance of viscous and capillary effects. In this problem, however, there is no extrinsic velocity and, if we replace U by its value at the lower edge, we find that the capillary number there, at time t, is given by

$$Ca = \frac{\mu a_0 \rho g a_0 \sin\theta}{\gamma \mu} \frac{\mathrm{d}a}{\mathrm{d}t} = \frac{1}{\sigma} \frac{\mathrm{d}a}{\mathrm{d}t}. \tag{23}$$

When the capillary number is large, we do not expect the contact lines and the dynamics of the fluid and free surface near them to have much effect on the motion. However, when the fluid elongates into the form of a thin sheet, we expect the velocity of the contact line to become small; the associated capillary number will also be reduced, so contact-line effects will eventually become important, even if they are not so initially.

3. Fluid sheet

In the experiments described by Huppert (1982), a fixed amount of fluid was placed uniformly across the plane and, when released, formed an elongating thin sheet of fluid with, at first, a straight leading edge. If there is no spanwise variation, and if, for the present, we ignore slip, the equation (19) for h reduces to the form

$$3\frac{\partial h}{\partial t} + \sigma \frac{\partial}{\partial x}\left(h^3 \frac{\partial^3 h}{\partial x^3}\right) - \cot\theta \frac{\partial}{\partial x}\left(h^3 \frac{\partial h}{\partial x}\right) + \frac{\partial}{\partial x} h^3 = 0. \tag{24}$$

When the transitory effects associated with the initial release of the fluid have disappeared, a similarity solution is possible in which the first and last terms of (24) are balanced, that is, the viscous stress on the plane balances the weight of the fluid and the fluid motion forces a change in the position of the free surface of the fluid.

This similarity solution was found by Huppert, and, in the notation used here, has the form

$$h = \frac{x^{\frac{1}{2}}}{t^{\frac{1}{3}}}. \tag{25}$$

With the upper edge of the fluid remaining at its initial position, the volume constraint (22) determines the position of the lower edge. We have, from (22) and (25),

$$\int_0^a h\,\mathrm{d}x = \frac{2a^{\frac{3}{2}}}{3t^{\frac{1}{3}}} = 1, \tag{26}$$

and so

$$a = \left(\frac{9t}{4}\right)^{\frac{1}{3}}, \tag{27}$$

In this solution, the height of the sheet increases down the sheet and reaches a maximum value proportional to $t^{-\frac{1}{3}}$ at its end, the length of the sheet being proportional to $t^{\frac{1}{3}}$. The relevance of this solution to his experiments was tested by Huppert, who found that it did describe the temporal development of the fluid sheet quite accurately.

If we compute the sizes of the neglected terms in (24), compared with the terms retained, we find that the approximation is valid provided that

$$\sigma \ll x^{\frac{5}{2}}t^{\frac{1}{3}}, \quad \cot\theta \ll x^{\frac{1}{2}}t^{\frac{1}{3}}, \tag{28}$$

and hence, for $t \gg 1$, the solution holds, except near the trailing edge. In addition, at the trailing edge, the slope of the free surface is infinite and the conditions of lubrication theory are violated. A more serious criticism of this solution is that the height of the sheet is $(2t/3)^{-\frac{1}{3}}$ at the lower edge of the sheet and not zero. Thus it is necessary to include short regions near the two edges in which surface tension is not negligible in order to complete the solution.

Near the trailing edge, which is fixed at $x = 0$, we can find another similarity solution, in which we can take h to have the form given by

$$h = t^{-\frac{2}{5}}f(\eta), \quad \eta = xt^{\frac{1}{5}}. \tag{29}$$

When this postulated form is substituted into (24), we find that f must satisfy the equation

$$\sigma(f^3f''')' + 3f^2f' + \tfrac{2}{5}(\eta f' - 3f) = 0, \tag{30}$$

to which the surface-tension term has contributed, while the other omitted term (with factor $\cot\theta$) is only $O(t^{-\frac{2}{5}})$ relative to the retained terms. The boundary conditions on f are that

$$f = 0 \quad \text{at} \quad \eta = 0; \quad f \sim \eta^{\frac{1}{2}} \quad \text{as} \quad \eta \to \infty. \tag{31}$$

A numerical calculation confirms that such a solution exists, with

$$f = 2.2\sigma^{-\frac{1}{5}}\eta + O(\eta^2 \ln\eta) \quad \text{for} \quad \eta \ll 1, \tag{32}$$

so that, at $x = 0$,

$$\frac{\partial h}{\partial x} = 2.2\sigma^{-\frac{1}{5}}t^{\frac{2}{5}}. \tag{33}$$

The slope at the upper edge is finite and decreases monotonically as time increases. When the slope falls below the value of β_s, the upper edge of the fluid will begin to slide down the plane. Of course, if $\beta_s = 0$ the upper edge will never move. We have,

therefore, completed the solution near the upper edge without altering the validity of the description of the motion of the bulk of the fluid provided by Huppert's similarity solution (25).

For the vicinity of the leading edge, we need a solution that will have a finite slope at the edge itself and match with the similarity solution away from it. A suitable form for this region is given by

$$h = t^{-\frac{1}{3}} f(\xi), \quad \text{where} \quad \xi = \sigma^{-\frac{1}{3}} t^{\frac{1}{9}} (a(t) - x). \tag{34}$$

The position of the edge is given by (27) and the boundary conditions for f are that $f \sim c\xi$ as $\xi \to 0$ for some constant c, and $f \to (\frac{3}{2})^{\frac{1}{3}}$ as $\xi \to \infty$ in order to match with (25) at $x = a$. For large t, the leading terms in (24) when h is given by (34) obey the equation

$$(f^3 f''')' - (f^3)' + (\tfrac{9}{4})^{\frac{1}{3}} f' = 0, \tag{35}$$

where a prime denotes a derivative with respect to ξ. The time-derivative term in (24) only contributes to this equation through the dependence of a on t, so this is a quasi-steady equation. The omitted terms are $O(t^{-\frac{2}{3}})$ compared with the terms forming (35). Huppert produced an equation similar to (35) and deduced the existence of a capillary region near the contact line in which the height of the drop increased from zero to match with his similarity solution away from the edge. However, his equation omitted the third term in (35) and the sign of the first term was reversed. We can integrate (35) once, to give

$$f^3 f''' - f^3 + (\tfrac{9}{4})^{\frac{1}{3}} f = C, \tag{36}$$

and C, the constant of integration, must be zero if f is to have the correct limit at infinity. Hence,

$$f^2 f''' = f^2 - (\tfrac{9}{4})^{\frac{1}{3}}. \tag{37}$$

The only solution of this equation that satisfies $f(0) = 0$ has the form

$$f = k\xi(-\ln \xi)^{\frac{1}{3}}. \tag{38}$$

Although this solution has an infinite slope at the origin, the singularity is only a weak one and the solution might be regarded as acceptable, if it were not for the fact that the constant k must be *negative*. The failure of this attempt to complete the similarity solution of Huppert by adding to it a narrow region near the edge where surface tension is important requires us either to abandon Huppert's solution or to modify the equations near the contact line. The first possibility conflicts with the experimental measurements made by Huppert, which confirmed the rate of extension of the sheet given by (27) very well. The alternative is to allow for slip near the edge; this should not cause any surprise since it is well known that difficulties arising from moving contact lines can be removed by such a modification.

With the slip included, the equation for h is given by (24) with h^3 replaced by $h^2(h+\lambda)$ and, with the same variable changes as before, (37) becomes

$$f(f + \lambda t^{\frac{1}{3}})(f''' - 1) = -(\tfrac{9}{4})^{\frac{1}{3}}, \tag{39}$$

provided $\lambda t^{\frac{1}{3}} = \epsilon \ll 1$, and we again have a quasi-steady solution. The boundary conditions that f must satisfy if it is to be a satisfactory representation of the free surface of the sheet near the leading edge are

$$f(0) = 0, \quad f'(0) = c, \quad f(\infty) = (\tfrac{3}{2})^{\frac{1}{3}} + O(\epsilon). \tag{40}$$

The small change in the value of f at infinity is of negligible significance and comes about because our model for slip allows it to be present everywhere and not just in

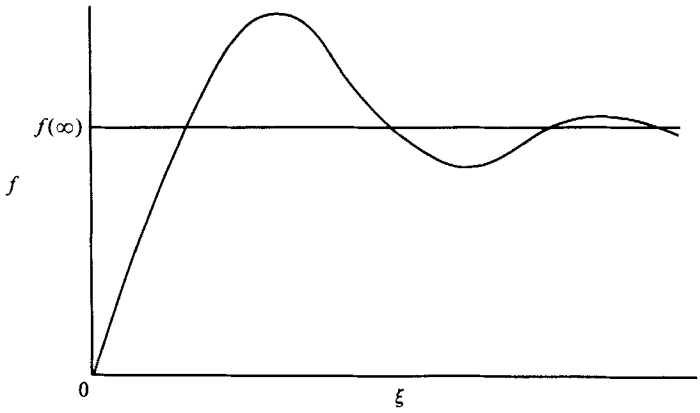

FIGURE 4. Height of the sheet near the leading edge.

the vicinity of the moving contact line. Since appropriate values of λ are exceedingly small this convenient assumption for the modification is acceptable.

A numerical solution of (39) confirms that a solution that satisfies the conditions (40) exists for all values of c. The structure of the solution can be divided into three parts. For values of ξ of order ϵ, f' increases to a large value, dependent on $-\ln\epsilon$. This is followed by a region in which ξ is of order 1 in which the value of f exceeds $f(\infty)$, rises to a maximum and then falls to values near $f(\infty)$. Finally, there is a long region in which f approaches its value at infinity in a damped oscillatory fashion. A sketch of this behaviour is drawn, not to scale, in figure 4. For the inner region, we can set

$$f = \epsilon(\tfrac{3}{2})^{\frac{1}{3}}F, \quad \xi = \epsilon X, \tag{41}$$

and to leading order (39) becomes

$$\frac{\mathrm{d}^3F}{\mathrm{d}X^3} = -\frac{1}{F(F+1)}. \tag{42}$$

For small values of X, the solution has the form

$$F = c_1X + O(-X^2\ln X), \tag{43}$$

and, for large X,

$$F \sim X(3\ln X + c_2)^{\frac{1}{3}}, \tag{44}$$

where c_1 and c_2 are constants. A solution asymptotically proportional to X^2 is possible, but gives a large positive value of f'' in the outer region, which implies that $f > f(\infty)$ for some finite value of ξ with f'' positive and increasing and it is impossible to match this solution to the required condition at infinity. In the outer variables, the solution (44) becomes

$$f \sim (\tfrac{3}{2})^{\frac{1}{3}}\xi(-3\ln\epsilon + c_2 + 3\ln\xi)^{\frac{1}{3}}, \tag{45}$$

and the boundary condition for the leading term in this region is

$$f'(0) = (-\tfrac{9}{2}\ln\epsilon)^{\frac{1}{3}} = d_1, \tag{46}$$

say. When $f \gg 1$, $f''' = 1$, from (39), so that

$$f = d_1\xi - \tfrac{1}{2}d_2\xi^2 + \tfrac{1}{6}\xi^3. \tag{47}$$

If d_2 has a value close to, but larger than, $(2d_1)^{\frac{1}{2}}$, f reaches a maximum value proportional to $d_1^{\frac{3}{2}}$ at a value of ξ proportional to $d_1^{\frac{1}{2}}$ before decreasing to a value $O(1)$.

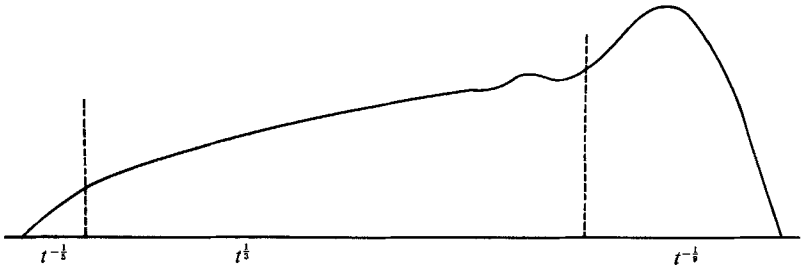

FIGURE 5. Profile of the elongated sheet before instability.

For the final stage, in which f approaches its asymptotic value, we can write $f = f(\infty)(1+g)$, where g is small, and (39) becomes

$$g''' = 2g, \tag{48}$$

confirming that g tends to zero in an oscillatory manner. This analytic description of the solution, without being complete, identifies the three regions suggested by the numerical work.

We have now shown that the similarity solution for the bulk of the elongating sheet of fluid can be satisfactorily matched with edge regions in which surface tension is important. The shape of the free surface for large t is sketched in figure 5. The most significant feature is the ridge near the leading edge, where the height of the sheet is considerably greater than that higher up the plane. In the ridge, as we have seen, there is a balance between gravity and surface tension, and the shape is the same as in a static fluid sheet. Figure 5 does not include the narrow slip region of width λ at the leading edge. The apparent contact angle, that is the slope of the surface at the edge, measured in the outer region, can be found from (46) and (34). We find that

$$\alpha_{\text{app}} = t^{-\frac{2}{5}}(-\tfrac{9}{2}\ln\epsilon)^{\frac{1}{3}}. \tag{49}$$

The speed of the contact line $\mathrm{d}a/\mathrm{d}t = \frac{1}{3}t^{-\frac{2}{3}}$, so that the apparent contact angle varies with the capillary number in the manner given by

$$\alpha_{\text{app}} = Ca^{\frac{1}{3}}(-\tfrac{27}{2}\ln\epsilon)^{\frac{1}{3}}. \tag{50}$$

This model therefore produces a dynamic variation in the contact angle measured outside the slip region. Of course, we cannot expect to obtain contact-angle hysteresis. The similarity solution ceases to be valid when the contact angle decreases to its maximum static value, since the contact line then stops moving. The dependence of the contact angle on the cube root of the capillary number agrees with the data on apparent contact angles obtained by Hoffman (1975), as was established by de Gennes (1985).

4. Instability of the elongating sheet

Now that we have found a description of the motion of the sheet of fluid, including the contributions made by surface tension at the two edges, we can try to find an explanation for the observed instability of the motion.

The basic similarity solution for the bulk of the sheet can be extended to permit

spanwise variations of the leading edge. The value of h is still given by (25), but the position of the lower edge can have the form

$$a(y,t) = A(y)\left(\frac{9t}{4}\right)^{\frac{1}{3}}, \tag{51}$$

provided A satisfies the volume condition

$$\int_0^d A^{\frac{3}{2}}\,\mathrm{d}y = d. \tag{52}$$

Hence, any initial disturbance of the leading edge is magnified as it advances down the plane by a factor proportional to $t^{\frac{1}{3}}$ without changing shape. This, however, does not have the features of the observed instability, which appeared spontaneously after the sheet had become sufficiently elongated. Also, surface tension does not play any role in the development of such a deformation of the leading edge, while the measured lengthscale of the spanwise variation was found to depend on the size of the surface tension.

In order to examine the evolution of a small spanwise corrugation of the surface of the sheet, we can write

$$h = \left(\frac{x}{t}\right)^{\frac{1}{2}}(1+\cos qy\, g(\xi)), \quad \xi = \frac{x}{t^{\frac{1}{3}}}, \tag{53}$$

where g is small. The relevant form of the general equation (19) for h, including the effect of the spanwise curvature of the surface, is

$$3\frac{\partial h}{\partial t}+\frac{\partial h^3}{\partial x}+\sigma\frac{\partial}{\partial y}\left(h^3\frac{\partial^3 h}{\partial y^3}\right)=0, \tag{54}$$

and when the value of h given by (53) is substituted, we obtain the equation

$$3g+\tfrac{2}{3}\xi\frac{\mathrm{d}g}{\mathrm{d}\xi}+\sigma q^4\xi^{\frac{3}{2}}g=0. \tag{55}$$

This equation has the solution

$$g = \xi^{-\frac{3}{4}}\exp\left(-\sigma q^4\xi^{\frac{3}{2}}\right), \tag{56}$$

so that the disturbance decays in the downward direction.

From these considerations, we deduce that the instability is closely connected with conditions near the leading edge of the sheet. Contact-line dynamics, and the associated capillarity and contact-angle phenomena, are usually only of prime importance when the capillary number is small. In Huppert's experiments the capillary number is initially large, but, as the fluid becomes elongated, the velocity decreases and so does the contemporary value of the capillary number. Precise values of the length of the sheet when the instability began are not given by Huppert, but he does provide a comparison between the experiments and the similarity solution, from which we can infer that the contact line is still straight when the capillary number has decreased to values of 0.05 or less. This strongly suggests that the cause of the instability must be sought in the low-capillary-number regime, which is consistent with its delayed appearance.

The shape of the surface of the sheet when it has become long, as sketched in figure 5, consists of a ridge of fluid near the lower edge, with a thinning sheet of fluid extending back to the upper edge. It does not seem likely that this sheet plays a

significant role in the instability. If this supposition is correct, we can consider, instead of the combined ridge and sheet, an isolated ridge of fluid, and yet retain the dynamical processes that are important in producing the observed fingers and triangles at the lower edge of the sheet.

5. Linear instability of a fluid ridge

The spreading and sliding of a ridge of fluid placed on an inclined plane with straight, horizontal contact lines, was considered by Hocking (1981, 1982). He showed that, to leading order, the shape of the ridge is given by a quasi-steady balance between gravity and surface tension. For a ridge of given width, the instantaneous contact angles cannot be predetermined and the motion of the ridge is driven by the necessity for the ridge to move so that the contact angles reach their proper values and that the net component of force on the fluid in the ridge down the plane is zero. To arrive at an evaluation of the speeds at which the two edges of the ridge move it is necessary to examine the slip regions near each edge and to match the solutions in these regions with the flow outside them. A similar approach for the present problem, in which the edges do not remain straight, would be more difficult. Instead, it seems legitimate to examine the stability of the ridge in its progress down the plane by postulating a convenient form for the dynamic variation in the contact angle. Then we can determine the instantaneous height of the ridge for given positions of the edges by the quasi-static balance of surface tension and gravity. This will enable us to find the contact angles at the edges and, from the known dependence of these angles on the velocity of the contact lines, we can advance the edges to the position they reach after a small time interval. Proceeding in this way, we can find the evolution of the positions of the edges of the ridge as the fluid moves down the plane.

The governing equations are given by (1)–(17), but it is convenient to change the non-dimensionalization. We choose as the lengthscale a_0, the half-width of the ridge in its initial position. We now define σ in terms of this lengthscale by

$$\sigma = \frac{6\gamma}{\rho g a_0^2 \sin\theta}, \tag{57}$$

and non-dimensional values of the height of the ridge, the time and the volume of the fluid in the ridge by

$$h' = \frac{h a_0}{\sigma}, \quad t' = t a_0 \sigma \delta', \quad V' = \frac{4a_0^3}{3\sigma} dV; \tag{58}$$

we also have to scale the static contact angles by writing

$$\alpha_s = \alpha_\sigma/\sigma, \quad \beta_s = \beta_\sigma/\sigma. \tag{59}$$

The leading term in the equation for h, which is a modified version of (19) using the new scalings, is given by

$$\frac{\partial}{\partial x}\left(\frac{\partial^2 h}{\partial x^2} + \frac{\partial^2 h}{\partial y^2}\right) + 6 = 0, \tag{60}$$

and this equation is to be solved in the region defined by

$$b(y,t) < x < a(y,t), \quad 0 < y < d, \tag{61}$$

with boundary conditions

$$h = 0 \quad \text{on} \quad x = b, a; \quad \frac{\partial h}{\partial y} = 0 \quad \text{on} \quad y = 0, d; \tag{62}$$

and with the volume constraint

$$\int_0^d \int_b^a h \, \mathrm{d}x \, \mathrm{d}y = \tfrac{4}{3} dV. \tag{63}$$

The normal velocity components at the edges are given by

$$U_a = \frac{\partial a}{\partial t}\left\{1 + \left(\frac{\partial a}{\partial y}\right)^2\right\}^{-\frac{1}{2}}, \quad U_b = \frac{\partial b}{\partial t}\left\{1 + \left(\frac{\partial b}{\partial y}\right)^2\right\}^{-\frac{1}{2}}, \tag{64}$$

and the angles between the free surface of the fluid and the plane at the contact lines are given by

$$\alpha = -\frac{\partial h}{\partial x}\bigg|_{x=a}\left\{1 + \left(\frac{\partial a}{\partial y}\right)^2\right\}^{\frac{1}{2}}, \quad \beta = \frac{\partial h}{\partial x}\bigg|_{x=b}\left\{1 + \left(\frac{\partial b}{\partial y}\right)^2\right\}^{\frac{1}{2}}. \tag{65}$$

The edge conditions (16) and (17), which determine the evolution of the positions of the edges, then become

$$\left.\begin{aligned} \alpha &= \alpha_\sigma + U_a, && \text{if } U_a > 0, \\ \beta_\sigma \leqslant \alpha &\leqslant \alpha_\sigma, && \text{if } U_a = 0, \\ \alpha &= \beta_\sigma + U_a, && \text{if } U_a < 0, \end{aligned}\right\} \tag{66}$$

for the lower edge, and

$$\left.\begin{aligned} \beta &= \beta_\sigma - U_b, && \text{if } U_b > 0, \\ \beta_\sigma \leqslant \beta &\leqslant \alpha_\sigma, && \text{if } U_b = 0, \\ \beta &= \alpha_\sigma - U_b, && \text{if } U_b < 0, \end{aligned}\right\} \tag{67}$$

for the upper edge. We must also have α and β non-negative.

At $t = 0$, the edges are given by $a(y, 0) = 1$, $b(y, 0) = -1$ and the solution of (60) that satisfies conditions (62) and (63) is

$$h = x - x^3 + V(1 - x^2), \quad \alpha = 2(1 + V), \quad \beta = 2(V - 1), \tag{68}$$

and we must have $V \geqslant 1$. This completes the formulation of the problem for the ridge of fluid on an inclined plane; the parameters are V, d, α_σ and β_σ.

We consider first the motion of the ridge with straight edges and then examine the stability of this motion to a small imposed spanwise variation of the edges of the ridge. It is convenient to take an origin moving with the centre of the ridge and so to write

$$a = a_\mathrm{c} + a_\mathrm{e}, \quad b = a_\mathrm{c} - a_\mathrm{e}, \quad x = a_\mathrm{c} + X, \tag{69}$$

with $a_\mathrm{c} = 0$, $a_\mathrm{e} = 1$ initially. The appropriate solution of (60) is then

$$h = (a_\mathrm{e}^2 - X^2)\left(X + \frac{V}{a_\mathrm{e}^3}\right), \quad \alpha = 2a_\mathrm{e}^2 + \frac{2V}{a_\mathrm{e}^2}, \quad \beta = -2a_\mathrm{e}^2 + \frac{2V}{a_\mathrm{e}^2}. \tag{70}$$

If both edges are moving down the plane, (66) and (67) show that

$$\frac{\mathrm{d}a_\mathrm{e}}{\mathrm{d}t} = \frac{2V}{a_\mathrm{e}^2} - \frac{\alpha + \beta}{2}, \quad \frac{\mathrm{d}a_\mathrm{c}}{\mathrm{d}t} = 2a_\mathrm{e}^2 - \frac{\alpha - \beta}{2}, \tag{71}$$

provided $V \geqslant 4a_e^4$. These two equations give the rates at which the ridge spreads and slides, respectively. A steady motion is possible, with a_e given by $a_e^2(\alpha+\beta)4V$, and with the ridge moving with the constant speed $\frac{1}{2}V(\alpha+\beta)-\frac{1}{2}(\alpha-\beta)$.

We now suppose that the edges are displaced by a small spanwise disturbance, so that their position is given by

$$a = a_c + a_e + \epsilon \cos qy\, a_q, \quad b = a_c - a_e + \epsilon \cos qy\, b_q, \tag{72}$$

where ϵ is small. If the ridge is unbounded in the spanwise direction, q is arbitrary, but, if it is bounded, the possible values of q are multiples of π/d. The height of the ridge is $h+\epsilon h_q$, where h is given by (70) and h_q, which is a harmonic function, has the form

$$h_q = \cos qy(A_q \cosh qX + B_q \sinh qX). \tag{73}$$

If we retain only the linear terms in an expansion in powers of the small parameter ϵ, the condition that the height should vanish at the edges gives the equations

$$\left.\begin{aligned} A_q \cosh qa_e &= a_e^2(a_q+b_q)+\frac{V}{a_e^2}(a_q-b_q), \\ B_q \sinh qa_e &= a_e^2(a_q-b_q)+\frac{V}{a_e^2}(a_q+b_q). \end{aligned}\right\} \tag{74}$$

The time-variations of a_q and b_q are fixed by the edge conditions (66) and (67), which, since we are assuming that both edges are moving, give the equations

$$\left.\begin{aligned} \frac{da_q}{dt} &= \left(6a_e+\frac{2V}{a_e^3}\right)a_q - q(A_q \sinh qa_e + B_q \cosh qa_e), \\ -\frac{db_q}{dt} &= \left(6a_e-\frac{2V}{a_e^3}\right)b_q - q(A_q \sinh qa_e - B_q \cosh qa_e). \end{aligned}\right\} \tag{75}$$

These equations have solutions proportional to $\exp(pt)$ with p given by

$$\frac{a_e^3}{2V}p = 1 - Q\coth 2Q \pm [Q^2 \operatorname{cosech}^2 2Q + P^2(9-6Q\coth 2Q+Q^2)]^{\frac{1}{2}}, \tag{76}$$

where $Q = qa_e$ and $P = a_e^4/V$. The condition that the slope at the upper edge must be non-negative shows that the permissible range for P is $0 \leqslant P \leqslant 1$. The amplitude of the distortions of the edges will grow with time when $p > 0$. For $P = 0$, the ridge is unstable when $Q\tanh Q < 1$, that is, when $0 < Q < 1.1997$, approximately. For $P = 1$, there is instability when $Q < 2\tanh 2Q$, that is, when $0 < Q < 1.9987$, approximately. The instability boundary for other values of P is sketched in figure 6. The maximum growth rate for each value of P occurs as $Q \to 0$, that is, for disturbances with the longest wavelength. In an unbounded channel, all we can say is that sufficiently long disturbances to the positions of the edges will grow; a nonlinear theory is needed to establish their shapes. For a channel of width d, the smallest possible value of Q is $\pi a_e/d$. If this value for Q lies on the stable side of the curve in figure 6, all disturbances to the edges will remain small and the ridge is stable. Otherwise, we expect disturbances with wavelength equal to $2d$ to grow most rapidly. If this disturbance remains the dominant one when the amplitude has become large, the edges will have their maximum displacement at one wall and their minimum at the other. Fluid from one half of the channel will drain towards the other half and the bulk of the fluid will move down the plane on that side.

Although we have established that a ridge of fluid, in a sufficiently wide channel,

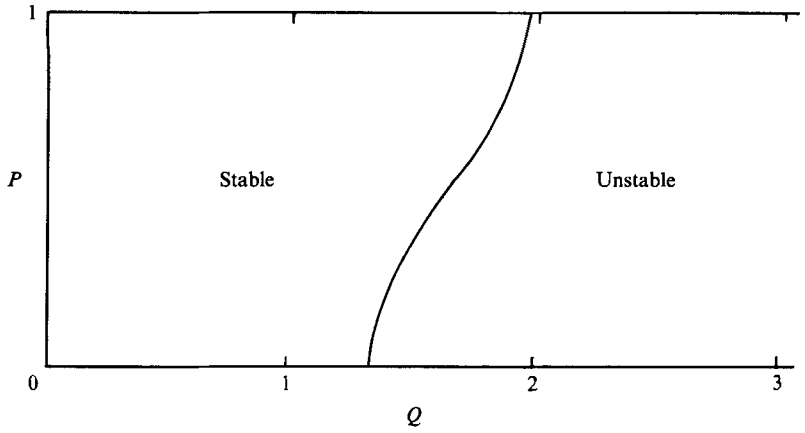

FIGURE 6. Linear stability boundary.

is unstable, the form that instability takes is not that observed experimentally. The observed fingers and triangles have a width which is much less than that of the channel. But in order to predict the shapes to which an initial disturbance of the edges may lead, linear instability analysis is not enough. A preliminary investigation of nonlinear affects is reported in the next section.

In the linear analysis, we have assumed that a_e is constant, although it will in general be a function of the time. The exception is the special case for which $a_e^2(\alpha+\beta) = 4V$ when the ridge slides without spreading. This neglect of the time-variation of the basic state in the perturbation analysis is justified if the growth rates of the instability are large. But in order to determine the nonlinear behaviour, this variation must be included and it is not sufficient simply to continue the expansion to higher powers of the amplitude ϵ, while keeping a_e constant.

6. Nonlinear instability of a ridge

For the nonlinear problem, we suppose that the edges are given an initial small displacement. For the unbounded case, this disturbance is assumed to be periodic and symmetric, so that the solution need only be found in a half-period. For the bounded case we can make a similar assumption, the half-period being then equal to the width of the channel. We ignore the effect of boundary layers on the walls of the channel. One computational method for the solution of this problem is to express the positions of the edges in the form of a Fourier series, namely

$$a = a_0 + \sum_1^\infty a_m(t)\cos\frac{m\pi y}{d}, \quad b = b_0 + \sum_1^\infty b_m(t)\cos\frac{m\pi y}{d}. \tag{77}$$

The height of the sheet can similarly be expressed in a form that satisfies (60), namely

$$h = -x^3 - Cx^2 + A_0 + B_0 x + \sum_1^\infty \left(A_m \cosh\frac{m\pi x}{d} + B_m \sinh\frac{m\pi x}{d}\right)\cos\frac{m\pi y}{d}. \tag{78}$$

If these expansions are truncated at $m = N$, we have $4N+5$ unknowns which can be found by collocation from the edge conditions $h = 0$ at $x = a, b$ at $N+1$ points along each edge, the contact-angle conditions (66) and (67) at the same points, and the volume constraint (63). The initial positions of the edges are given by $a = 1$ and

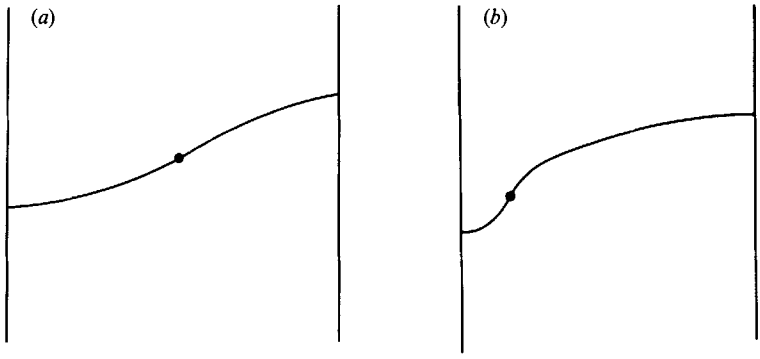

FIGURE 7. Nonlinear evolution of the lower edge. The position of the inflexion point is marked. (a) Small amplitude. (b) Larger amplitude.

$b = -1$, with some small disturbance added. In the calculations reported here, the initial value of a was changed to 1.1 at one of the collocation points. This choice has the advantage that it does not favour a particular wavelength.

This numerical scheme was found to work satisfactorily for a limited time. As the ridge moves down the plane, the hyperbolic functions in (78) have to be evaluated for large arguments, particularly for the larger values of m, and this leads to an ill-conditioned matrix. The calculations could be performed for a longer time by using a moving origin midway between the mean positions of the two edges, but this too broke down when the range of values of a and b across the channel became large. Nevertheless, the results that were obtained enable certain conclusions to be reached. When the channel was narrow, the initial disturbance died away and the edges of the ridge remained straight as it moved down the plane, as predicted by the linear theory in §5. For larger values of d, the edges showed the half-wave shape as predicted, but as the amplitude grew the width of the lower portion of the fluid narrowed. A suitable measure of the width of this bulge was found by the distance of a point of inflexion of the edge from the channel wall. This bulge suggests the incipient appearance of a finger of fluid, although the calculations failed before that could be fully realized. An interesting feature of the calculations was that, when they were repeated with a channel of double the width, the width, and indeed the shape, of the bulge did not change. A sketch of the developing shape of the lower edge is shown in figure 7. This suggests that the nonlinear development of the shape of the edge of the fluid is into fingers whose width is independent of the channel width. When a disturbance was initiated on both sides of the channel, two such fingers of equal width developed, which points to the possibility of fingers with variable spacing, as in figure 1(*g*) of Huppert's (1982) paper. No suggestion of the observed triangular shapes was found in the calculations. The spanwise lengthscale for the instability was found experimentally to be proportional to $\gamma^{\frac{1}{3}}$, where γ is the surface tension. With the non-dimensionalization used here, this lengthscale could depend on d, the width of the channel, and on the scaled angles α_σ and β_σ, which are proportional to γ. The linear theory of §5 predicted that the spanwise length should be proportional to d, but the nonlinear calculations gave values independent of d and they were not in disagreement with the observed proportionality to $\gamma^{\frac{1}{3}}$.

7. Conclusions

The two-dimensional elongation and subsequent instability of a fluid sheet being stretched by gravity down an inclined plane has been investigated in this paper. The aim has been to describe the motion of such a sheet as observed by Huppert (1982) and to understand the appearance and subsequent growth of spanwise distortions of the initially straight leading edge of the sheet. In giving a summary of what has been done, it is convenient to compare the contents of this paper both with the observations recorded by Huppert, and with the quantitative results and explanations he deduces from them. Four goals for the investigation were identified in §1, and the extent to which each has been achieved can be described in turn.

The first goal relates to the growth of the sheet for that period in which the leading edge remains straight. The similarity solution derived by Huppert, and confirmed experimentally, has been completed by the inclusion of surface tension. This enables the solution to be found in the regions near both the stationary trailing edge and the moving leading edge. Because of the presence of a moving contact line, it is essential to remove the force singularity that occurs there when the no-slip condition is used. Huppert's attempt to close his similarity solution by including surface tension in the frontal region has been shown to be incorrect. A feature of the solution near the leading edge is an increase in the thickness of the fluid behind the front above that of the sheet extending up the plane to the trailing edge.

The second goal is to explain the delayed appearance of the instability that distorts the shape of the leading edge of the sheet. From his experiments, Huppert deduces that the length of the sheet when instability sets in is proportional to the square root of the cross-sectional area of the fluid which formed the sheet, but this is immediately obvious when the variables of the problem are made non-dimensional, as in §2. He claims that viscous effects would stabilize any cross-flow variations in the thickness of the sheet, so surface tension must be taken into account. However, it has been shown in §4 that surface tension is not destabilizing in the main part of the sheet and, if it is the cause of the instability, it must be because of its influence on the frontal region. Huppert himself relates the wavelength of the instability to the lengthscale of the frontal region, which depends on the surface tension through the non-dimensional parameter $\sigma^{\frac{1}{3}}$ (in the notation of the present paper), but he makes no attempt to explain the cause or the delay of the instability. From his experiments, however, it is clear that the instability only occurs when the capillary number has become sufficiently small and that it is the frontal region, and not the body of the sheet, that is significant in the appearance of the instability. If this is so, the motion in the frontal region must be determined accurately if any progress is to be made towards understanding the phenomenon, which requires contact-line and contact-angle effects to be incorporated.

The third goal is to predict theoretically the linear characteristics of the instability. This is a very difficult task, even numerically, because the base flow on which perturbations should be imposed is itself varying in both space and time. Since the main change in the profile of the sheet when the capillary number becomes small is the appearance of a ridge immediately behind the leading edge, a possible way forward is to concentrate on a model problem that consists of the ridge by itself. The base flow is then the quasi-steady sliding of the ridge down the plane, and a perturbation analysis is much easier to perform. This is done in §5, and the ridge is shown to be unstable to spanwise disturbance of sufficiently large wavelength. Of course, this model does not reproduce all the characteristics of the instability of the

sheet. The main difference is that in the model problem all disturbances are suppressed until the ridge has been fully developed and only then are perturbations allowed to occur. For the sheet, disturbances are free to occur at all times and may well begin to develop before the ridge is fully formed. This may well account for a major difference between the instability of the ridge and that observed in the sheet. For the ridge, no preferred wavelength is predicted, only a cut-off value dependent on the width of the container. The experiments, however, are reported to reveal a periodic shape for the leading edge, with the wavelength a constant multiple of $\sigma^{\frac{1}{3}}$; the scaling of this wavelength is fixed by dimensional analysis and the size of the frontal region or ridge. Examination of the photographs reproduced by Huppert shows that the shape is not precisely periodic and, in one case at least, is very far from being periodic (figure 1*g* in his paper).

The fourth goal concerns the nonlinear development of the instability. The appearance of triangles and fingers as the leading edge of the sheet advances is perhaps the most intriguing aspect of the instability, but no explanation of this phenomenon has yet been given. Since the linear theory does not determine a preferred wavelength, it is necessary to perform a nonlinear calculation before predictions can be made on the shape taken by the leading edge after the instability sets in. The preliminary numerical work for the ridge suggests the emergence of fingers of constant width, spaced irregularly, which is similar to the pattern shown in the cited figure of Huppert.

The final question that is natural to ask, but difficult to answer, concerns the physical reason for the instability. Huppert does not give an answer to this question, beyond the statement that surface tension is important. Since the motion is driven by gravity and influenced by surface tension, the basic mechanism may be the same as in Rayleigh–Taylor instability, modified by the controlling effects of the contact line and contact angle.

This paper was completed while I was at the Engineering Science and Applied Mathematics Department of Northwestern University. My visit there was supported by a grant from the US Department of Energy, reference DE-FG02-88ER13927.

REFERENCES

Dussan V., E. B. 1976 *J. Fluid Mech.* **77**, 665–684.

Dussan V., E. B. 1979 *Ann. Rev. Fluid Mech.* **11**, 371–400.

Dussan V., E. B. & Chow, R. T.-P. 1983 *J. Fluid Mech.* **137**, 1–29.

Gennes, P. G. de 1985 *Rev. Mod. Phys.* **57**, 827–863.

Hocking, L. M. 1981 *Q. J. Mech. Appl. Maths* **34**, 37–55.

Hocking, L. M. 1982 *Proc. 2nd Intl Coll. on Drops and Bubbles*, pp. 315–321. JPL Pub. 82-7, NASA/JPL.

Hocking, L. M. 1983 *Q. J. Mech. Appl. Maths* **36**, 55–69.

Hoffman, R. L. 1975 *J. Colloid Interface Sci.* **50**, 228–241.

Huppert, H. E. 1982 *Nature* **300**, 427–429.

Silvi, N. & Dussan V., E. B. 1985 *Phys. Fluids* **28**, 5–7.